

Effects of annealing and impurities on tensile properties of electrodeposited nanocrystalline Ni

Y.M. Wang ^{a,*}, S. Cheng ^b, Q.M. Wei ^c, E. Ma ^b, T.G. Nieh ^a, A. Hamza ^a

^a Lawrence Livermore National Laboratory, Chemistry and Materials Science Directorate, Livermore, CA 94550, USA

^b Department of Materials Science and Engineering, Johns Hopkins University, Baltimore, MD 21218, USA

^c Department of Mechanical Engineering, Johns Hopkins University, Baltimore, MD 21218, USA

Received 23 June 2004; received in revised form 13 August 2004; accepted 17 August 2004

Abstract

The strength of electrodeposited nanocrystalline Ni increased rather than decreased after annealing for 1 h at temperatures below 150°C, with little change in the grain sizes or detectable impurity segregation. Annealing at 200°C can be utilized to tailor the grain size distribution for improved ductility in combination with good strength. Further annealing at above 250°C, however, induced a transition to brittle behavior due to impurity segregation to grain boundaries concurrent with grain growth.

© 2004 Acta Materialia Inc. Published by Elsevier Ltd. All rights reserved.

Keywords: Nanocrystalline Ni; Mechanical property; Annealing; Impurity; Grain growth

1. Introduction

Electrodeposited nanocrystalline (nc) nickel has been used as a model material to investigate the mechanical behavior and deformation mechanism of nanocrystalline metals [1–4]. Different from nc materials prepared by several other fabrication techniques, electrodeposited nc metals are considered fully dense with truly nc grain sizes and fairly narrow grain size distributions. Such samples are desirable in order to understand the intrinsic mechanical behavior of nc metals. In addition, the samples prepared by the electrodeposition technique are sufficiently large for tensile tests, making them even more attractive for mechanical property studies.

However, contamination from the ingredients in the electroplating bath is a long-standing issue. The impurities incorporated into the deposits can include sulfur, nitrogen, oxygen, hydrogen and some metallic elements

that come from bath additives such as coumarin or saccharin as well as from anode materials [5]. Although the impurities have been measured for electrodeposited nc and ultrafine-grained metals [1,6], their effects on mechanical behavior remain poorly understood. It is often assumed that the impurities are uniformly distributed in the as-deposited sample at too low concentrations to be of a major concern, but will segregate to grain boundaries upon thermal annealing to affect mechanical properties [7]. As a result, the impurity effects are likely to couple with the history of thermal treatments. Recent molecular dynamics (MD) simulations [8], on the other hand, suggest that the grain boundaries of as-prepared nc grain boundaries are often in a non-equilibrium state, and thermal annealing may lead to the relaxation of the grain boundary structures, which, in turn, will affect the mechanical properties as well.

The annealing effects on the mechanical behavior of nanostructured metals have been studied previously in particulars produced by severe plastic deformation and inert gas condensation techniques [9,10]. These

* Corresponding author. Tel.: +1 925 422 6083; fax: +1 925 422 4665.

E-mail address: ymwang@llnl.gov (Y.M. Wang).

experiments suggest that depending on the annealing temperatures and durations, a simultaneous increase of the strength and ductility is achievable in nanocrystalline materials [9,10]. Because of impurity concerns, such annealing experiments have not been systemically carried out in electroplated nc metals. There are reports about the microstructure change and sulfur segregation in electrodeposited nc Ni during static thermal annealing [11,12], but these annealing experiments were mainly performed at rather high temperatures ($>400^{\circ}\text{C}$) where late stage abnormal grain growth occurred in nc Ni. It was shown that segregation of impurities occurred together with abnormal grain growth, with the sulfur concentration reaching as high as 5–11wt.% in the grain boundaries [7,11]. It is not clear thus far whether the redistribution of these impurities can happen at much lower temperatures and how that affects the mechanical properties. The purpose of this study is to investigate the effects of annealing at relatively low temperatures on the microstructures and impurity redistribution, and on the subsequent mechanical properties. The results on electroplated nc Ni are expected to be helpful for the interpretation of the deformation behavior of nanocrystalline metals.

2. Experimental

The electrodeposited nanocrystalline nickel was acquired from Integran Technologies Inc. (Canada). We used the same batch of the samples as those reported in Ref. [4]. The as-received nc Ni was quoted to have a nominal grain size of 15 nm and a thickness of $\sim 150\mu\text{m}$.

The tensile specimens with a gauge length of 5 mm and a width of 1.8 mm were cut using an electro-discharging machine and then heat treated in a vacuum (better than 1×10^{-3} Pa) oven for an hour at a temperature in the range of $50\text{--}300^{\circ}\text{C}$. After heat treatment, the surface layers on both sides were removed by polishing with silicon carbide papers of 400, 600, 800, 1200 metallurgical grits and alumina suspensions of 0.5 and $0.1\mu\text{m}$. The final thickness of the samples is about $120\mu\text{m}$. The tensile tests were carried out at room temperature and a strain rate of $1 \times 10^{-4}\text{s}^{-1}$ with a load cell resolution of 0.1 N. The data were recorded at a speed of one point per second.

A JEOL JXA-8200 electron microprobe operating at 15 kV was used to quantify the impurities in the as-received nc Ni. The electron beam size was $20\mu\text{m}$. The grain size and microstrain in the as-received and heat-treated samples were characterized by means of X-ray diffraction (XRD) and transmission electron microscopy (TEM). XRD was carried out on a Philips X'pert Pro MPD X-ray diffractometer using Cu- K_{α} radiation at an acceleration voltage of 45 keV and a current of

40 mA. The peak profile was analyzed based on the Scherrer–Wilson equation, using a custom-built Matlab program. To obtain the grain size distribution and the local impurity information in the samples, the microstructures of all samples were also characterized using a Philips CM-300 transmission electron microscope operating at 300 kV, equipped with an Oxford energy dispersive X-ray (EDX) detector and a Gatan image filter system for electron energy loss spectrometry (EELS) elemental mapping. The extraction voltage for the field-emission gun was 4.2 keV. TEM samples were prepared by double-jet electropolishing with electrolytic bath of 25% nitric acid and 75% methanol at a temperature below -30°C .

3. Results and discussion

3.1. Microstructural characterization

Table 1 lists the impurities and detection limit of each element in the as-received nc Ni. For comparison, the result of a standard high-purity Ni (99.999%), obtained using the same technique, is also included in the table. The electrodeposited nc Ni shows relatively high contents of carbon, sulfur and cobalt. The carbon and sulfur mainly originate from bath additives such as saccharin ($\text{C}_7\text{H}_4\text{NO}_3\text{S}$) used in the electrodeposition, whereas metallic impurities such as cobalt may come from the anode material. Hydrogen may also be present, but was not detectable using our technique. Compared with chemical analysis results reported for other electrodeposited nc Ni [1], the impurity contents are different in the current sample, which is not surprising as these materials were from different sources and the impurity contents are batch-dependent [1].

Fig. 1 shows the plan-view TEM micrographs and their corresponding statistical grain size distribution plots of the nc Ni, as-received and annealed at 100, 200, and 300°C , respectively. From the statistical size

Table 1
Compositional analysis result for as-deposited nanocrystalline nickel

Element	As-deposited nc-Ni (ppm)	Reference Ni (99.999%, ppm)	Detection limit (ppm)
Si	<	<	30
Fe	160	<	40
Al	10	20	10
Mn	<	<	35
S	460	10	10
Co	270	<	38
W	<	<	211
Mo	150	30	30
Zn	<	<	37
C	1820	<	10
N	<	<	350
O	50	<	50

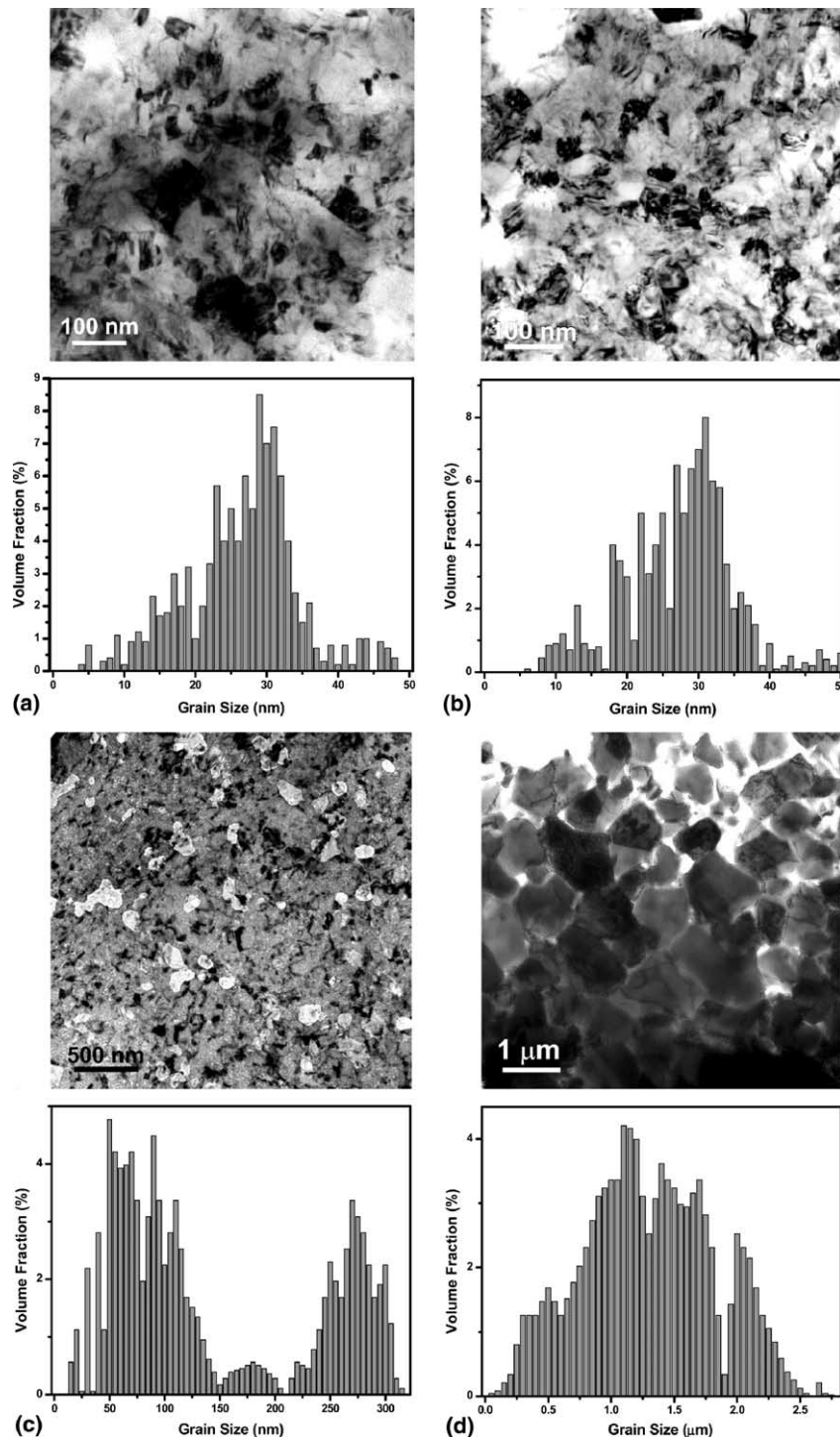


Fig. 1. Plan-view TEM bright-field images and statistical grain size distributions of (a) as-deposited, (b) 100 °C annealed, (c) 200 °C annealed, and (d) 300 °C annealed electrodeposited nc nickel. Grain growth is observable for the samples annealed at 200 °C and above. All the grain size distribution plots were obtained by counting at least 251 grains.

distribution plots of the grains observed in the TEM, the actual grain size averages around 29 nm in the as-received state, and changes only slightly to 31 nm after annealing at 100 °C. Abnormal grain growth was observed for annealing at 200 °C, the microstructure of which is characterized by a bimodal distribution with

some larger grains up to 300 nm surrounded by nanometer-sized grains [13–15], Fig. 1c. EDX of the 200 °C-annealed sample did not pick up marked sulfur segregation along the grain boundaries, suggesting that either the sulfur has not started to segregate or it is below the EDX detection limit (~ 0.5 wt.%). Further

Table 2

XRD analysis results on as-deposited and annealed nanocrystalline nickel

	Mean microstrain $\langle \epsilon^2 \rangle^{1/2}$ (%)	Average grain size
As-deposited nc-Ni	0.313 ± 0.005	29 ± 8
100 °C annealed nc-Ni	0.211 ± 0.006	31 ± 6

annealing at 300 °C caused the growth of most grains to the range of 1–2 μm . The bright contrast around the grain boundaries in Fig. 1d is due to preferential etching during TEM sample preparation, implying that the chemical composition of the grain boundaries became very different from that of the grain interior.

Because of the little difference seen in TEM between the as-received and 100 °C-annealed samples, XRD is used to analyze the average grain sizes and microstrains in these two samples. As shown in Table 2, the average grain size obtained from XRD peak broadening is 29 and 31 nm for the as-received and 100 °C-annealed samples, respectively, in reasonable agreement with the TEM measurements. XRD also indicates a reduction of microstrain from about 0.31–0.21% after 100 °C annealing, suggesting the occurrence of recovery in the samples.

3.2. Mechanical behavior

The microhardness values and tensile engineering stress–strain curves of the nc Ni before and after thermal annealing are shown in Fig. 2. To avoid the overlapping of multiple stress–strain curves, the tensile plots were displaced along the X-axis for clarity. The microhardness initially increases slightly, and then decreases sharply as grain growth sets in at higher annealing temperatures (≥ 200 °C). A relatively large error bar was measured for the sample annealed at 300 °C, as microcracks were often observed during indentations, suggesting the brittleness of the sample. The heat treatment also had pronounced effects on the yield stress (σ_y), ultimate tensile strength (σ_{UTS}), and tensile elongation to failure (ϵ_{TEF}) of the electrodeposited Ni, which are quantitatively listed in Table 3. In general, the tensile strength of our as-received sample is similar to those in Ref. [1] measured with large sample dimensions, so is the hardness value. For all other samples, the tensile behavior can be divided into three different regions according to the annealing temperatures.

Region I: annealing at low temperatures ≤ 150 °C. The most striking feature after annealing in this temperature region is the increase of the yield stress and ultimate tensile strength (see Table 3), consistent with the microhardness data. Interestingly, there is no obvious reduction of the total elongation to failure (1–3%). *This is the first time that such a behavior is observed for an electrodeposited nc metal.* Valiev et al. reported that

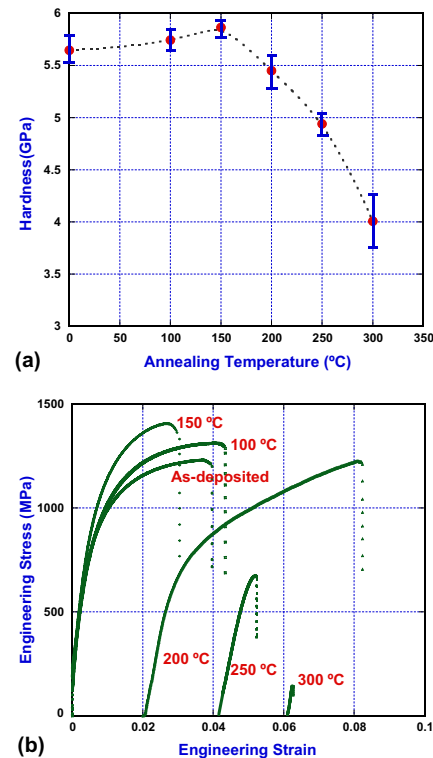


Fig. 2. (a) Room-temperature microhardness as a function of annealing temperature, and (b) room-temperature tensile engineering stress–strain curves of the electrodeposited nc nickel at a strain rate of $1 \times 10^{-4} \text{ s}^{-1}$. The hardness data were acquired using a Tribo-nanointenter with a diamond Berkovich tip.

Table 3

Engineering yield strength σ_y (0.2% offset), ultimate tensile strength (σ_{UTS}), and percentage tensile elongation to failure (ϵ_{TEF} %) of as-deposited and annealed electrodeposited nickel

Annealing temperature	σ_y (MPa)	σ_{UTS} (MPa)	ϵ_{TEF} (%)
As-deposited	839	1233	3.0
100 °C	856	1312	3.3
150 °C	920	1406	2.0
200 °C	604	1221	7.1
250 °C	603	672	0.3
300 °C	—	141	0

thermal annealing led to an increase of the yield stress in nanostructured Ti prepared by the severe plastic deformation (SPD) technique [9]. However, the grain size in Ref. [9] is on the 100 nm level, beyond the limit of nanocrystalline regime. Also, the SPD materials are known to contain excess amounts of dislocations at the grain boundaries. It is thus not clear if this phenomenon is common in nc metals. Weertman et al. prepared truly nc metals using the inert gas condensation of powders and observed microhardness increase after annealing [10]. But there the cause of strengthening can be simply attributed to densification (reduced porosity) of the consolidated samples during heat treatment.

Electroplated nc Ni is considered fully dense with only minor micro- and nano-scale pores [5], therefore it is unlikely that the density change is the sole cause for the notable strengthening upon thermal annealing. The redistribution of the trace amounts of impurities may have some effects on the strength, but it was not detected (by EDX). There is, however, a measurable (by XRD) microstrain reduction after annealing. This is indicative of (grain boundary) dislocation reorganization activities. A recent MD simulation suggests that thermal annealing can lead to strengthening of nc metals due to relaxation at the non-equilibrium grain boundaries. The rationale is that it would become more difficult for such relaxed grain boundaries to emit dislocations or undergo grain boundary sliding, thus making the material more resistant to yielding under applied stresses [8]. Note that this is a behavior opposite to that of conventional pure metals, where annealing always lowers the strength due to the reduction of dislocation density. In an nc metal, the intra-grain dislocation sources easily available in conventional metals are not present. Some “easier” dislocation sources at the grain boundaries can be removed by a moderate annealing, leading to strength elevation as a result of the depletion of available dislocation sources.

Region II: annealing at temperatures $\sim 200^\circ\text{C}$. Moderate grain growth was observed, resulting in a decrease of the yield stress but an increase of the tensile ductility to $\sim 7\%$. Here again, impurity segregation remained below the detection limit of EDX, which explains why the samples annealed in this temperature region gain better ductility [7]. This result suggests a way to achieve a good combination of strength and ductility in electrodeposited nc metals. The idea of using a bimodal grain distribution developed during annealing to optimize tensile properties has never been tried on an electrodeposited nc metal before [13].

Regions III: annealing at temperatures $\geq 250^\circ\text{C}$. Here grain growth becomes significant. As the diffusivity of sulfur in Ni is several orders higher than the self-diffusivity of Ni at these annealing temperatures [7], S and impurities similar to S are expected to segregate to the much smaller number of grain boundaries of larger grains. As expected, this adversely affects the tensile properties. In spite of the micrometer-sized grain sizes developed after annealing, the Ni samples now exhibit brittle behavior. The fracture stress of the annealing materials also decreases with increasing temperatures. Such a transition from ductile to brittle behavior is confirmed by examining the fracture surfaces of the tested samples, Fig. 3. Both the as-deposited and low-temperature annealed samples clearly exhibit ductile features with dimple sizes several times larger than the grain sizes. But when the annealing temperature surpassed 250°C , a fracture surface characterized by intergranular cleavage was observed.

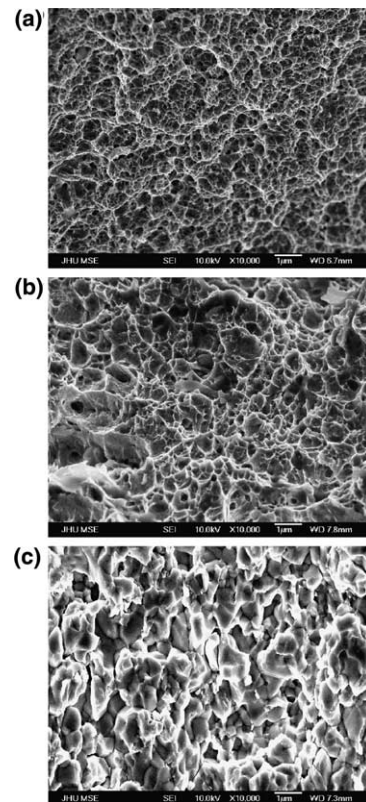


Fig. 3. SEM fractographs of (a) as-deposited, (b) 150°C annealed, and (c) 300°C annealed Ni samples. The fracture surfaces of all the samples annealed below 200°C show ductile dimple features similar to (a) and (b). The intergranular cleavage failure features of (c) were observed for the samples annealed above 250°C .

Heuer et al. has studied the effect of sulfur segregation to grain boundaries on the intergranular embrittlement behavior of conventional coarse-grained Ni [7]. They also observed a transition to brittle behavior, when

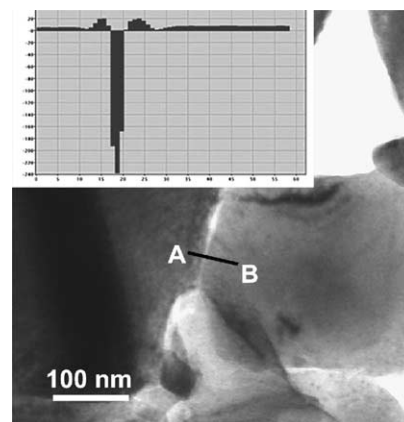


Fig. 4. TEM image of 300°C annealed electrodeposited nickel. The inset shows the EELS elemental mapping signal using sulfur L edge along the line AB. The segregation of sulfur at the grain boundary is evident.

the sulfur concentration reached 15.5 ± 3.4 at.% (6.9–11 wt.%). As shown in Fig. 4, our EELS elemental mapping using sulfur L edge evidently resolved a high concentration of S on the grain boundaries. Further EDX with a beam size of 5 nm focused on the grain boundaries indicates that in some places the sulfur content reaches as high as 6.3 wt.%, which is close to the value reported by Heuer et al. This explains the dramatic embrittlement of electrodeposited nickel at room temperature after annealing at relatively low temperatures. A similar concentration of sulfur along the grain boundaries has also been reported by Hibbard et al. in an electrodeposited nickel annealed at 420 °C [11], and by Weertman [16], although they did not report mechanical property data. Finally, it is noteworthy to point out that the observed embrittlement was not caused by carbon redistribution, as our EELS elemental mapping did not detect any obvious segregation of carbon into grain boundaries.

The S segregation and the resulting brittle behavior suggests that for electroplated nc metals, care must be taken to set limits for the annealing parameters when developing a grain size distribution to improve ductility (as discussed for Regime II), or when using annealing to obtain coarse-grained reference samples. Our new results suggest that the impurity segregation could happen at much lower temperatures (~ 250 °C) than those reported in the literature [7,11,12].

4. Summary

After mild annealing at several temperatures (50–300 °C for 1 h), electrodeposited nc Ni exhibited significantly different microstructures and tensile properties. Caution should be exercised to take thermal history and impurity segregation into account [17], when investigating/designing/comparing the mechanical properties of electrodeposited nanocrystalline metals.

- (1) We showed a way to improve the tensile properties of electroplated nc Ni through low-temperature annealing. An increase of the hardness, yield stress and fracture stress was observed after heating at a temperature < 150 °C, with no observable impurity segregation or reduction in ductility. We also discussed a possible mechanism for the annealing-induced strengthening [8,9].
- (2) A bimodal grain structure was developed at the intermediate annealing temperature (200 °C) with impurity segregation remaining undetectable. A

combination of decent strength and ductility can be reached for carefully selected annealing parameters [13].

- (3) However, for annealing temperatures higher than ~ 250 °C, tensile ductility can be completely lost notwithstanding much increased grain sizes. The transition to brittle behavior is believed to originate from the segregation of sulfur detected at grain boundaries. This calls into question the practice of annealing electrodeposited nc metals to modify grain sizes for comparative studies, and the interpretation of deformation behavior at elevated temperatures without considering impurity segregation.

Acknowledgments

The authors thank Prof. T.C. Hufnagel for providing the program for fitting XRD patterns. Part of this work was performed under the auspices of the US Department of Energy by University of California, Lawrence Livermore National Laboratory under Contract W-7405-Eng-48. YMW gratefully acknowledges the support of Graboske Fellowship. EM and SC acknowledge the support of National Science Foundation, DMR-0355395.

References

- [1] Dalla Torre F, Van Swygenhoven H, Victoria M. *Acta Mater* 2002;50:3957.
- [2] Kumar KS, Suresh S, Chisholm MF, Horton JA, Wang P. *Acta Mater* 2003;51:387.
- [3] Budrovic Z, Van Swygenhoven H, Derlet PM, Van Petegem S, Schmitt B. *Science* 2004;304:273.
- [4] Wang YM, Ma E. *Appl Phys Lett* 2004, in press.
- [5] Kumar KS, Van Swygenhoven H, Suresh S. *Acta Mater* 2003;51:5743.
- [6] Lu L, Shen Y, Chen X, Qian L, Lu K. *Science* 2004;304:422.
- [7] Heuer JK, Okamoto PR, Lam NQ, Stubbins JF. *Appl Phys Lett* 2000;76:3403.
- [8] Hasnaoui A, Van Swygenhoven H, Derlet PM. *Acta Mater* 2002;50:3927.
- [9] Valiev RZ, Sergueeva, Mukherjee AK. *Scripta Mater* 2003;49:669.
- [10] Weertman JR, Sanders PG. *Solid State Phenom* 1994;35–36:249.
- [11] Hibbard GD, McCrea JL, Palumbo G, Aust KT, Erb U. *Scripta Mater* 2002;47:83.
- [12] Xiao C, Mirshams RA, Whang SH, Yin WM. *Mater Sci Eng A* 2001;301:35.
- [13] Wang YM, Chen MW, Zhou F, Ma E. *Nature* 2002;419:912.
- [14] McFadden SX, Mishra RS, Valiev RZ, Zhilyaev AP, Mukherjee AK. *Nature* 1999;398:684.
- [15] Wang N, Wang Z, Aust KT, Erb U. *Acta Mater* 1997;45:1655.
- [16] Weertman JR. Private communication, 2004.
- [17] Van Swygenhoven H. Private communication, 2004.